

# The effects of deposition conditions on microstructure and magnetic properties of TbFeCo

J-W. Lee, H-P. D. Shieh, M. H. Kryder, and D. E. Laughlin

Magnetics Technology Center, Carnegie Mellon University, Pittsburgh, Pennsylvania 15213

Transmission electron microscopy (TEM) has been employed to characterize micro/magnetic structural details of magneto-optical (MO) recording TbFeCo thin films as a function of dc-magnetron sputtering parameters using bright/dark field imaging, selected area diffraction, convergent beam electron diffraction, and Lorentz electron microscopy. It is found that the preparation conditions have a strong impact on both microstructure and magnetic properties of the films. The microstructures of the films deposited at low argon bleeding pressures ( $< 10$  mTorr) are featureless, and their magnetic domains are of the "stripe" type with a perpendicular anisotropy. In contrast, high argon pressures ( $> 20$  mTorr) give rise to microvoids surrounding "honeycomblike" networks and in-plane domains with "ripple type" contrast. The microstructure and magnetic domain structures are related to the films' magnetic properties as characterized by a MO loop tracer.

## I. INTRODUCTION

Tb-Fe-Co amorphous thin films have been studied extensively as a promising candidate for magneto-optical (MO) recording media because of their perpendicular magnetic anisotropy as well as their high readout signal-to-noise ratio.<sup>1,2</sup> It is known that perpendicular magnetic anisotropy is closely associated with micro/magnetic structures which depend on deposition parameters such as argon pressure ( $P_{Ar}$ ) and substrate bias voltage ( $V_b$ ). The investigation of structural changes in Tb-Fe-Co has been reported as a function of  $P_{Ar}$ <sup>3</sup> and of oblique incidence angle.<sup>4</sup> However, few attempts have been made to correlate the micro/magnetic structural changes with magnetic properties of sputtered Tb-Fe-Co films as a function of deposition parameters. Hence, this paper describes further results of micro/magnetic structural changes and magnetic properties in Tb-Fe-Co films as a function of  $P_{Ar}$ .

## II. EXPERIMENT

The films were prepared from a FeCo based Tb-Fe-Co mosaic target by a dc-magnetron sputtering system on carbon-coated Cu grids for direct observation by transmission electron microscopy (TEM).<sup>5</sup> They also were deposited on glass substrates for cross-sectional TEM observation and magneto-optical (MO) measurements. The sputtering was carried out at the following  $P_{Ar}$ : 2, 10, 20, and 40 mTorr. The deposition rate at cathode power density of  $2.2 \text{ W/cm}^2$  was  $120 \text{ nm/min}$  and the nominal area composition of the target was  $\text{Tb}_{27}(\text{Fe}_4\text{Co}_1)_{73}$ . The nominal thickness of the films is  $50 \text{ nm}$ . TEM was performed using a Philips EM420T analytical electron microscope. The magnetic domain structures were observed by the Fresnel mode imaging in Lorentz electron microscopy (LEM) at  $120 \text{ kV}$ . The MO hysteresis loops were measured through the glass substrate of films at room temperature with a  $633\text{-nm}$  He-Ne laser in fields up to  $7 \text{ kOe}$ .

## III. RESULTS AND DISCUSSION

Transmission electron micrographs of plane view and cross-sectional specimens of Tb-Fe-Co films deposited at

four different  $P_{Ar}$  are shown in Figs. 1 and 2. The structures change with  $P_{Ar}$  reflecting a variation in the mechanism by which the film grows. In Fig. 1(a) ( $P_{Ar} = 2$  mTorr), the film structure is shown to be relatively smooth and featureless. At  $10$  mTorr, the film morphology is even smoother [Fig. 1(b)]. As the  $P_{Ar}$  increases further ( $20$  mTorr), the morphologies change in that the film now contains microvoids surrounding amorphous islands [Fig. 1(c)]. Further increase in  $P_{Ar}$  ( $40$  mTorr) leads to a large increase in the density of microvoids [Fig. 1(d)].

Cross-sectional samples also reveal smooth and featureless morphologies for films deposited at lower  $P_{Ar}$ , i.e.,  $2$  and  $10$  mTorr [Figs. 2(a) and 2(b)]. Also, the microvoids are observed to be perpendicular to the film plane at higher  $P_{Ar}$ ; i.e.,  $20$  and  $40$  mTorr [Figs. 2(c) and 2(d)]. The smooth morphology at lower  $P_{Ar}$  and the high density of perpendicular microvoids causing a columnar microstructure at higher  $P_{Ar}$  are consistent with the zone model proposed by Thornton.<sup>6</sup>

Figures 3 and 4 are selected area diffraction (SAD) and convergent beam electron diffraction (CBED) patterns, respectively. At low  $P_{Ar}$  ( $2$  mTorr), the SAD pattern exhibits a broad halo [Fig. 3(a)]. Similarly, the CBED pattern reveals only one broad halo [Fig. 4(a)]. It should be noted, however, that the halo in the CBED pattern appears to contain weak spots (arrowed). This may indicate that the amorphous phase coexists with microcrystals. With increasing

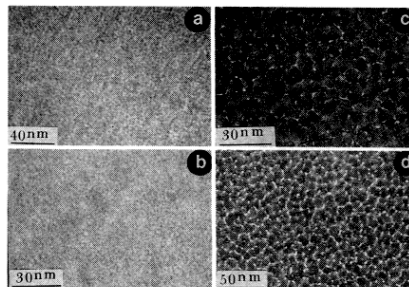


FIG. 1. Bright field TEM images of Tb-Fe-Co films (plane view): (a) 2, (b) 10, (c) 20, and (d) 40 mTorr.

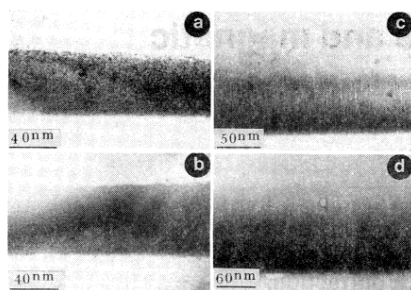


FIG. 2. Bright field TEM images of cross-sectioned Tb-Fe-Co films: (a) 2, (b) 10, (c) 20, and (d) 40 mTorr.

$P_{Ar}$  (10 mTorr), the SAD pattern shows one broad halo as well as the weak contrast of a second halo [Fig. 3(b)]. The corresponding CBED pattern contains only one halo [Fig. 4(b)]. However, the CBED pattern still displays weak spots within the halo. At 20 mTorr  $P_{Ar}$ , the contrast of the second halo becomes stronger [Fig. 3(c)], as do the microcrystalline reflections within the first halo [arrowed in Fig. 4(c)]. As the  $P_{Ar}$  increases even further (40 mTorr), the same observation can be made as shown in Figs. 3(c) and 4(c) [see Figs. 3(d) and 4(d)]. These results suggest that the films contain microcrystals. The size of the crystals is less than 1.5 nm. In addition, as the  $P_{Ar}$  increases, the number of microcrystals appears to increase.

The presence of the crystalline reflections could be due to either oxides of the rare earth element Tb or microcrystals of the ternary alloy. However, Tb oxides have larger  $d$  spacings<sup>7</sup> than the spacings that we observe in SAD patterns. This rules out the interpretation of the reflections as “oxides.” Experimentally, it has been confirmed<sup>8</sup> that “the increase in  $P_{Ar}$  increases the exit temperature of the deposited metal, i.e., 64 °C at 1 mTorr  $P_{Ar}$  and 106 °C at 25 mTorr  $P_{Ar}$ .” Thus the crystallization of the amorphous phase is more likely to occur at higher argon pressure. This inference is consistent with our results since the increasing  $P_{Ar}$  leads to sharper contrast of microcrystalline reflections.

Figure 5 reveals that the magnetic domain structures of films is dependent upon  $P_{Ar}$ . At 2 mTorr  $P_{Ar}$ , the domains are “stripe type” associated with white and black dots typical of perpendicular magnetization [Fig. 5(a)]. Increasing  $P_{Ar}$  to 10 mTorr [Fig. 5(b)] does not significantly change the domain configurations. However, the domain width in-

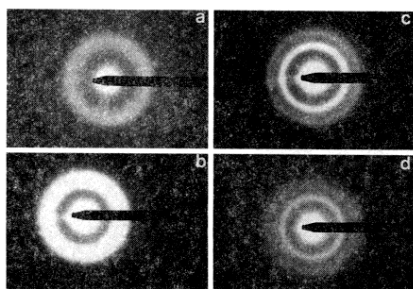


FIG. 3. SAD patterns of Tb-Fe-Co films: (a) 2, (b) 10, (c) 20, and (d) 40 mTorr.

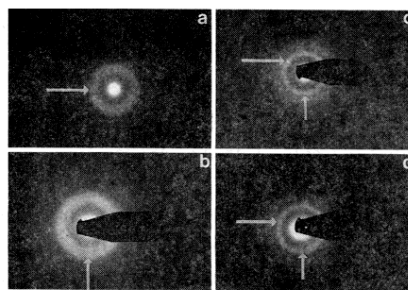


FIG. 4. CBED patterns of Tb-Fe-Co films: (a) 2, (b) 10, (c) 20, and (d) 40 mTorr.

creases, showing more widely spaced black and white domains. As the  $P_{Ar}$  increases further (20 mTorr), the domain structures exhibit a “featherlike” ripple configuration associated with small domains containing an in-plane component of magnetization [Fig. 5(c)]. However, a few white and black dots associated with a perpendicular component of magnetization remain. Thus, at larger  $P_{Ar}$ , a greater amount of in-plane magnetization exists even though the microstructure is more columnar. This suggests that the columnar microstructure is not the major cause of perpendicular anisotropy. Furthermore, the decrease of perpendicular magnetization is not unexpected with increasing  $P_{Ar}$  since the microstructures show a high density of microvoids as well as a higher number of microcrystals.

At 40 mTorr, one cannot see any evidence for the formation of domains [Fig. 5(d)]. This may be associated with deposition parameters. Results (Figs. 1 and 2) indicate that the increase in  $P_{Ar}$  increases the density of microvoids. Oxygen may react with Tb along the microvoids to form non-magnetic oxides. Thus the oxides may shield the magnetic portions of the amorphous phases. This leads to further separation between magnetic portions so that the interaction energy between the magnetic regions is greatly reduced. This reduction in interaction energy would give rise to a low magnetization and hence weak Lorentz force, not capable of producing images in LEM.<sup>9</sup>

The influence on the perpendicular magnetization of  $P_{Ar}$  shown in Fig. 5 can also be observed through MO hysteresis loops. At 2 and 10 mTorr [Figs. 6(a) and 6(b)], the loops are rectangular, typical of materials with an easy axis normal to the film plane. Further increase in  $P_{Ar}$

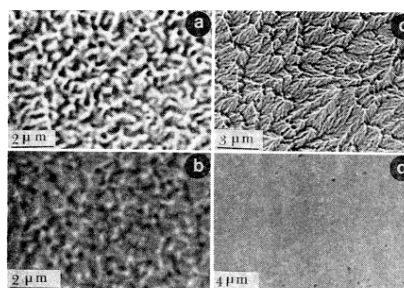


FIG. 5. Lorentz images of Tb-Fe-Co films: (a) 2, (b) 10, (c) 20, and (d) 40 mTorr.

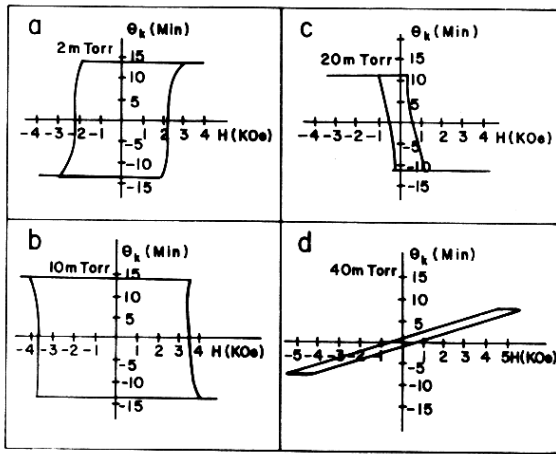


FIG. 6. MO hysteresis loops of Tb-Fe-Co films: (a) 2, (b) 10, (c) 20, and (d) 40 mTorr.

(20 mTorr) decreases the coercivity to 0.7 kOe. At 40 mTorr, the loop becomes sheared (squareness < 1) indicating that the film is dominated by in-plane magnetization components.

#### IV. CONCLUSIONS

(1) Low  $P_{Ar}$  produces films with microstructures that are smooth and featureless while high  $P_{Ar}$  produces films with microvoids surrounding the amorphous islands.

(2) Films grown at high  $P_{Ar}$  contain columnar shape morphologies.

(3) It is suggested that TbFeCo films contain a mixture of amorphous and microcrystalline (< 1.5 nm) phases.

(4) At low  $P_{Ar}$ , the films show "stripe type" magnetic domains associated with white and black dotted domains. In-plane "featherlike" domains are observed at high  $P_{Ar}$ .

(5) MO loops indicate that low  $P_{Ar}$  gives rise to perpendicular magnetization while higher  $P_{Ar}$  is dominated by in-plane magnetization.

#### ACKNOWLEDGMENTS

This research was funded in part by International Business Machines Corporation (IBM) and also supported by the Magnetic Materials Research Group at Carnegie Mellon University, Pittsburgh, PA 15213, through the Division of Materials Research, National Science Foundation, under Grant No. DMR-8613386. One of the authors (H-P.D. Shieh) would like to acknowledge the support of an IBM post-doctoral fellowship.

<sup>1</sup>Y. Togami, K. Kobayashi, M. Kajimura, K. Sato, and T. Teranishi, *J. Appl. Phys.* **53**, 2334 (1982).

<sup>2</sup>F. Tanaka, Y. Nagao, and N. Imamura, *IEEE Trans. Magn.* **MAG-20**, 1033 (1984).

<sup>3</sup>M. Hong, E. M. Gyorgy, R. B. van Dover, S. Nakahara, D. D. Bacon, and P. K. Gallaghen, *J. Appl. Phys.* **59**, 551 (1986).

<sup>4</sup>S.-C. Shin, *J. Appl. Phys.* **61**, 3340 (1987).

<sup>5</sup>H-P. D. Shieh, M. Hong, and S. Nakahara (these proceedings).

<sup>6</sup>J. A. Thornton, *J. Vac. Sci. Technol.* **11**, 666 (1974).

<sup>7</sup>S. Nakahara, M. Hong, R. B. van Dover, E. M. Gyorgy, and D. D. Bacon, *J. Vac. Sci. Technol.* **A4**, 543 (1986).

<sup>8</sup>D. P. Ravipati, W. G. Heines, and J. L. Dockendorf, *J. Vac. Sci. Technol.* **A 5**, 1968 (1987).

<sup>9</sup>T. Chen and G. B. Charlan, *J. Appl. Phys.* **50**, 4285 (1979).